

Simulation of the Docking Phase for the SMART-OLEV Satellite Servicing Mission

Clemens Kaiser, Peter Rank
Kayser-Threde GmbH
clemens.kaiser@kayser-threde.com

Rainer Krenn, Klaus Landzettel
German Aerospace Center, DLR
rainer.krenn@dlr.de

Abstract

Satellite servicing in GEO in terms of fleet management and life extension is going to be an important element in the telecom satellite operations business from the commercial point of view. The SMART-OLEV (Orbital Live Extension Vehicle) mission concept is based on a chaser satellite that docks at a client satellite and takes over the AOCS-tasks of the mated configuration and/or performs orbital manoeuvres. The most critical phase within this mission will be the (soft-)docking of both satellites. Extensive simulations of this phase have been performed in order to detect critical issues of the docking strategy and to verify the technical feasibility of the mission. The applied models cover the dynamics of the satellites and their AOCS as well as the applied docking sensors and tools. The FEM-inspired Polygonal Contact Model was used for high fidelity simulation of the physical contact between the satellites. Concluding the docking simulations could successfully support the OLEV-project to achieve the status ready to continue for phases C/D.

1. Introduction

SMART-OLEV will provide life extension and other services from 2010 onwards for geostationary communications satellites suffering from propellant depletion or having anomalies in the AOCS or propulsion subsystem, and even recovery from launch failures will be possible [1]. The satellite works as an Orbit Life Extension Vehicle using the SMART-1 platform heritage (Figure 1). A contract has been signed in summer 2007 with one of the large satellite operators as launching customer for the OLEV service.

SMART-OLEV will use a purpose designed and built spacecraft to mechanically dock with a client satellite's zenith face using its liquid apogee engine nozzle and launch vehicle interface ring. No electrical connections are necessary. SMART-OLEV will take

over attitude and orbit control functions for the client satellite allowing the client to continue to operate the other functions on the communication satellite as normal. In this way valuable geostationary hardware and orbital slots can be maintained and secured in a very cost effective manner.

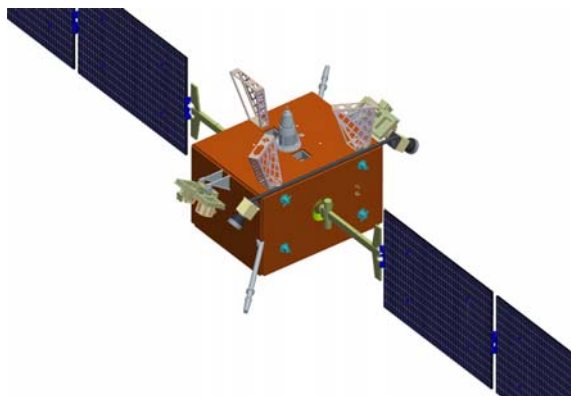


Figure 1: SMART-OLEV Spacecraft

SMART-OLEV will be controlled before and during docking from a dedicated Operations Control Center (OCC). After docking, attitude and orbit control may be transferred to the client's OCC if desired. Orbital Satellites Services Limited (OSSL) is the customer's interface point commercializing the offered on-orbit services and in charge to sign the contracts with the customers – primarily the telecom satellite operators. OSSL itself takes care of the launch services and insurances. The design and development of the complete OLEV space and ground system is a European Partnership program with an industrial consortium consisting of Swedish Space Corporation, Kayser-Threde and Sener with support by national space agencies and the European space agency as well as further co-funding sources.

The SMART-OLEV is a further development of the former CX-OLEV™ spacecraft using now a flight proven platform technology to limit the development

cost. The program is still open for further industrial partners taking over responsibility of platform or payload subsystems following a stringent commercial path to realize the first and following missions. It is planned to perform a PDR begin of 2008 and to start the Phase C/D activities in spring 2008. Goal is to have the docking in space to the first client in 2011.

2. Rendezvous & Docking Overview

Rendezvous with the client satellite takes a few days and can occur anywhere within the geostationary arc but not 24 h a day due to specific illumination needed by the sun. SMART-OLEV and the client satellite will be tracked from the ground to within 1 km of each other. Far field cameras will then guide the spacecraft to within 5 meters of the client satellite by manoeuvring SMART-OLEV via a series of “stationary points” using the reaction control subsystem. Command, tracking and real time telemetry will be via the dedicated OCC and Ground Station with image data being received by ground stations within the PrioraNet global network. An overview of the complete Rendezvous and Docking strategy is shown in Figure 2.

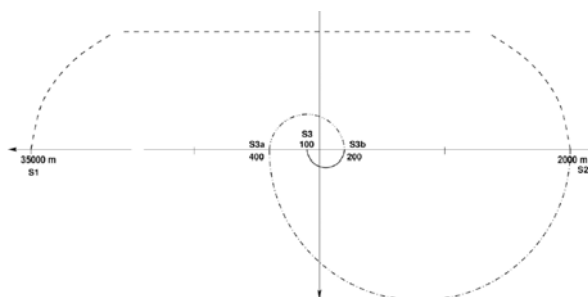


Figure 2: Rendezvous Strategy

2.1. Approach

Starting from the “rendezvous point” SMART-OLEV approaches to the “parking position” according to a pre-defined speed profile (speed as a function of the distance in x direction) kept on the Data Handling System (DHS). The distance to the client is calculated on ground using the stereo images of the Docking Payload cameras and provided to SMART-OLEV. The target illumination and the camera exposure times may be adapted to the changing illumination conditions using ground commands.

2.2. Insertion

On ground command the boom is deployed with constant speed. Before the first sensor plane of the Capture Tool enters the nozzle, the ground operator has to enable the capturing at the RVD Payload Control Unit (DPCU, the command to enable the capturing may be issued in an earlier (sub-) phase either, e.g. before the docking phase is started). When the capturing is enabled, the DPCU S/W monitors the distance sensors selected in order to detect the insertion of the first sensor plane into the nozzle. When the plane has entered, the transition into the capturing sub-phase is initiated autonomously by the DPCU S/W.

2.3. Capturing

The DPCU S/W performs the autonomous activities described in the following. The displacement vector (relative position of client in y- and z-direction) is calculated from the distance sensor data and provided to the DHS. On basis of the distance vector and the nozzle profile the penetration depth is determined. The boom speed is varied according to the penetration depth and the distance of the Capture Tool tip to the nozzle wall. Furthermore the contact switches of the Capture Tool are monitored. When the contact switches indicate that the tip is fully inserted into the nozzle, the crown locking mechanism of the Capture Tool is activated and the provision of the displacement vector as well as the boom movement are stopped. This automatically terminates the capturing sub-phase.

2.4. Coupling

After the client is locked, the boom is commanded to retract. During retraction the boom speed may be adapted on command. When the client pushes onto the Client Support Brackets, the boom retraction is autonomously stopped. By means of a dedicated command the boom is slowly retracted in small steps, until the required boom tension is achieved. In this way the nominal mated configuration is established and the RVD P/L can be powered off.

3. Rendezvous & Docking Payload

The Rendezvous and Docking Payload for SMART-OLEV comprises a capture tool, deployment/retraction mechanisms, client support brackets, a target illumination system, a camera system (to be used for the complete RVD process) and their associated electronics subsystems.

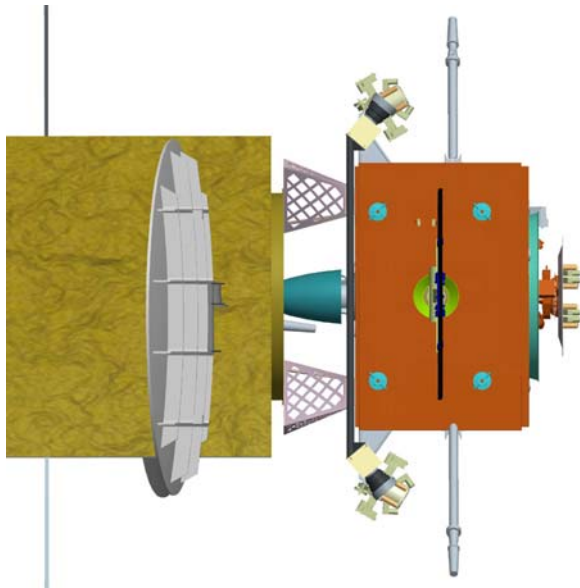


Figure 3: OLEV docked with Client Satellite

Kayser-Threde as Rendezvous and Docking Payload Prime Contractor is responsible for industrializing the DLR docking technology and the development and integration of the other elements. The payload is compatible with multiple docking and undocking operations thus maximizing the operational flexibility. In addition to that Kayser-Threde is also responsible for the respective ground system called Payload Control System (PCS) as part of the overall OLEV ground system from which all RVD operations will be controlled. Main element of the PCS is an image processing algorithm for both rendezvous and docking. For the rendezvous operations Sener is responsible for a full autonomous software program able to manoeuvre SMART-OLEV from the Rendezvous Point to the Parking Position.

The RVD Payload consists of the following components:

- A Capture Tool (CT) for capturing the target spacecrafts apogee engine nozzle. This is based on an existing development by DLR Institute of Robotics and Mechatronics and incorporates two planes of sensors for close proximity operations using different measuring principles (laser and inductive). Once within the engine injector, the capture tool uses a crown locking mechanism to maintain contact. The capture tool is able to cope with a wide variety of nozzle types and throat sizes.
- A Deployment/Retraction Mechanism (CDM), which extends and retracts a rigid metallic, spindle upon which the capture tool is mounted. Actuation is by electric motors and the capture tool can be extended and retracted approximately 0.7 meters.

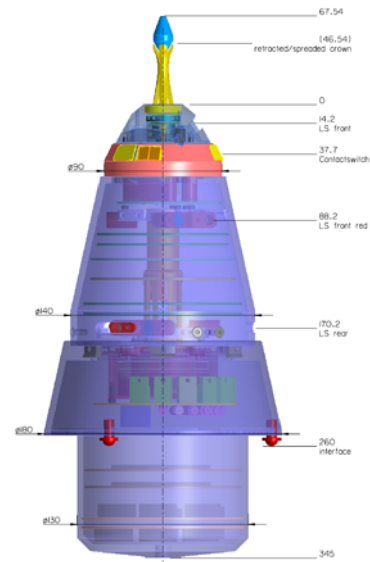


Figure 4: Capture Tool

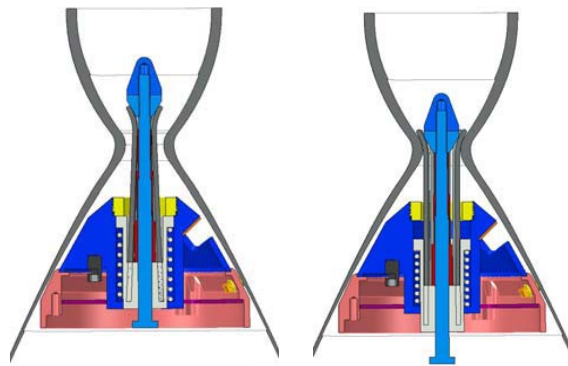


Figure 5: Locking Crown

- A Vision system for visual guidance during final approach from 5 meters. It consists of stereo camera and lighting to illuminate the client satellite when in shadow or within the apogee engine nozzle.
- Client Support Brackets (CSB). The client spacecraft is pulled down by the Capture Tool onto three supports located on SMART-OLEV top panel and compatibility with all three (937, 1194 and 1666 mm) interface rings.
- A Rendezvous and Docking Payload Control Unit (DPCU) for command and telemetry, control and power conditioning for the payload. This also includes an LEON3 processor. Final approach and docking will be performed by automated systems and software using stereo video and proximity sensor data fully backed up by an on ground operator.
 - After docking, contact pressure will be maintained at the interface via springs in the deployment/retraction

mechanism which react against the client support mechanisms. Undocking requires that the tension and crown locks be released and SMART-OLEV backs away from the client satellite.

4. DSF - Design Simulation Facility

To perform feasibility and design analysis in phases A/B for OLEV projects, a Design Simulator Facility (DSF) was developed and applied. The DSF for SMART-OLEV is currently maintained by Sener and serves as a common platform for all SMART-OLEV related simulations to be performed by the participating parties.

With help of specific docking simulations a number of crucial questions regarding feasibility of docking and mission success had to be answered:

- Is the approach strategy as proposed for OLEV suitable in terms of satellite control and operation of the docking payload?
- Is the accuracy of the applied sensors sufficient for the proposed control algorithm and is it possible to extract the desired information from the according sensor data?
- Are the performances of the applied actuators and tools adequate for the dynamics of the system?
- Is there any danger for damaging the client satellite or the chaser satellite itself when physical contact between the docking payload and the client satellite and nozzle takes place?
- How does the client satellite reacts when having contact? What strategy shall be used to manipulate the client's AOCS to ease the docking process?

In order to be able to answer these kinds of questions the Design Simulator Facility has been equipped with a high fidelity contact dynamics model by DLR that is able to reproduce the characteristics, the amount and the impact direction of the applied contact forces during the physical contact phases of the docking operation.

4.1. Contact Dynamics Model for DSF

The contact dynamics models that have been implemented in DSF are derived from the so-called Polygonal Contact Model (PCM, [2]) and adapted to the particular application inside the simulator. The general idea of PCM is based on three major steps:

1. Discretization of the contact body surface by polygon meshes and assignment of contact relevant geometric and dynamics parameters individually to each polygon.

2. Detection of polygons, which are in contact with their counter part.
3. Calculation of contact forces/torques based on the relative kinematics states of the contact polygons under respect of the assigned geometric and dynamics parameters.

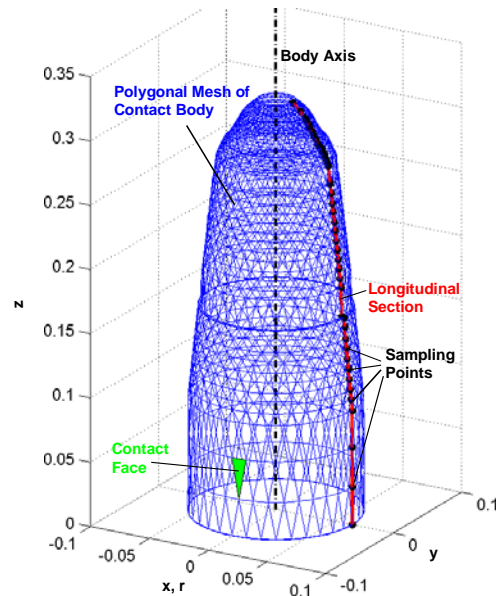


Figure 6: Contact Shape Definition

4.1.1. Contact Surface – Physical Properties

The method of creating the polygon meshes takes advantage of the fact that only rotationally symmetric surfaces are involved in contact dynamics events (Figure 6). Thus, they can be described by their discrete longitudinal section functions (radius versus axial co-ordinate), which may be also a function of further parameters in case of a variable surface shape. The distribution of the sampling points depends on the particular curvature of the longitudinal section function, respectively on the curvature of the body surface: The stronger the curvature, the shorter the distance of the sampling points. These settings guarantee for good sensitivity of the models regarding contact detection at a minimum number of surface polygons. The polygon mesh, respectively its vertices can be created by rotating the longitudinal section around the body axis with discrete angular distances. Within the polygon mesh three adjoining vertices define a so-called face (isosceles triangle).

After creating the discrete description of the body surfaces we can assign parameters, which are required for contact dynamics calculations, individually to each polygon face. The first set of parameter consists of

geometric properties Face size A , Face normal vector \mathbf{n} and Face center co-ordinates \mathbf{C} .

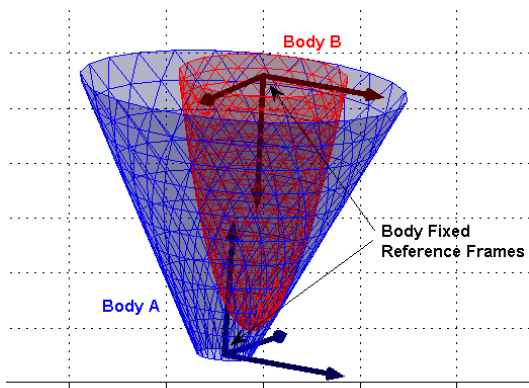


Figure 7: Contact Shape Definition

In the second parameter set the dynamic properties will be assigned. Here, each polygon face is interpreted as linear spring-damper system acting in its individual face normal direction. Thus, we assign individual stiffness and damping coefficients c and d . This approach is modeling the surface stiffness as well as energy dissipation during contact. The physics of Coulomb friction between the surface polygons is represented by individual friction coefficients μ for both, stick and slip states.

4.1.2. Contact Detection – Contact Shape

In order to detect, if a body surface is intersecting the surface of its reference body (e.g. Body B intersecting Body A, Figure 7), the according polygon vertex co-ordinates of the inspected body have to be transformed into the body fixed reference frame of the reference body as visualized in. In the second step we can map all vertices into a two-dimensional reference frame of radial and axial co-ordinates.

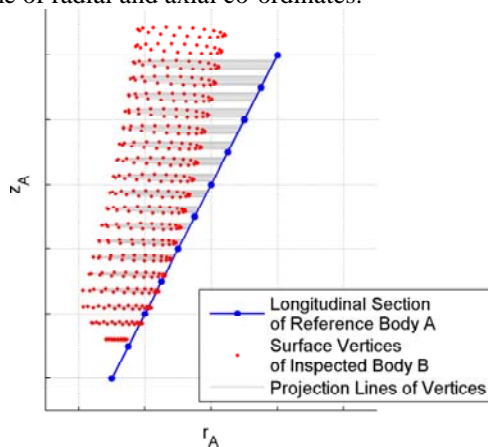


Figure 8: 2D-Projection of Vertices and Contact Detection (Radial)

Herein the reference body appears as its own longitudinal section. And following we can compare the radial co-ordinates of the vertices of the inspected body just with the longitudinal section function of the reference body in order to decide about contact or not contact (Figure 8). From the computation point of view this algorithm is very time-efficient since the number of matrix operation can be reduced drastically compared to contact detection in the three-dimensional space. Moreover, the method can be applied to contact dynamics problems including convex bodies as well as concave bodies and it doesn't cause any limitation in terms of multi-point contact configurations.

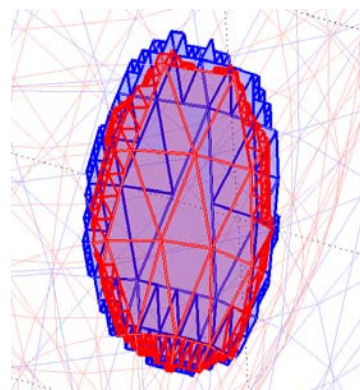


Figure 9: 3D Contact Shape With Border Refinement

After re-mapping of those vertices, which are actually in contact, into the 3D space we are able to define the contact shape by the according polygon mesh grid (Figure 9). Ambiguous solutions at the border of the contact shape (only one or two vertices of the face in contact) will be fixed by a refinement of the regarding polygons and the repetition of the contact detection in an iterative process. This refinement option inside the model is essential since the ambiguous solution is much more likely during running simulations than the unambiguous one (all vertices or none of the vertices of a face in contact).

4.1.3. Relative Motion States of Contact Surfaces

Further components for the contact force calculation are the relative motion states of the contact shape polygons, strictly speaking the polygon centers C relative to their counterparts. The required motion states are the normal penetration depth of the contact polygon into the counterpart polygon s , the normal penetration velocity v_n and the relative tangential velocity between the contact polygon center w.r.t. the surface of the counterpart v_t . The counterpart polygons can be found by mapping (radial projection)

the contact shape polygons onto the surface of the reference body (Figure 10).

The relative motion states between two counteracting polygons can be easily found, first by calculation of their absolute motion states based on the absolute motion states of the contact bodies they belong to (model input parameter) and secondly by subtraction of the absolute values.

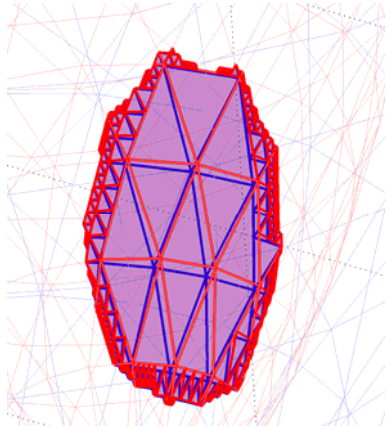


Figure 10: Mapped Reference Shape of Contact Shape

4.1.4. Contact Forces

With the pre-requisites, which were introduced in the previous chapters, namely the dynamics parameters of the polygons and the current relative kinematics states, we are able to calculate the actual contact forces, individually for each contact polygon by the sum of the following components (for simplification reasons only as scalar description):

- Normal force due to surface stiffness: $F_c = c \cdot s$.
- Normal force due to damping: $F_d = d \cdot v_n$.
- Tangential force due to Coulomb friction: $F_\mu = \mu(F_c + F_d)$.

The total contact force applied to the contact bodies will be calculated by integration over all polygons of the contact shape.

In the implementation for DSF the presented contact model (contact detection and contact force calculation) was done twice while in the second one the roles of inspected body and reference body were permuted. This procedure guarantees for the correct contact detection independent from the relative position of the contact bodies. However, caused by the differences in the discrete contact surface resolution as documented in Figure 9 the actual contact forces would slightly differ from each other. In order to be compliant with Newton's third law of motion (actio = reactio) we apply the mean value of both computations as the final contact forces.

4.2. Docking Simulations

This chapter focuses on the simulation results of the most critical phase of the docking operation that takes about two minutes. In this phase the Capture Tool

1. gets in physical contact with the client nozzle,
2. passes the nozzle throat,
3. opens its Locking Crown,
4. locks the client nozzle and
5. starts to retract the client satellite.

The contact sensitive bodies were

- the client nozzle,
- the Capture Tool body and
- the Locking Crown, which could change its shape in terms of length and diameter during simulation.

The simulations were performed as pure dynamics simulations in the three-dimensional space without any kinematics constraints or simplifications. Therefore, it is assumed that the reliability of the simulation results is sufficient for an assessment in terms of satellite docking success. Docking Simulation Scenario

The simulation scenario supposes a R-bar docking procedure in GEO (Figure 2). The initial position of the chaser satellite is the so-called parking position while limit cycling at a distance of about 20-30 cm away from the client nozzle rim. The initial misalignment between the Capture Tool axis and the nozzle axis is supposed to be 3 cm with equal components in V-bar and H-bar direction (Figure 11) as a worst case assumption. OLEV is controlled by its AOCS, the controller part of the client AOCS is switched off and the FMW are controlled at constant speed waiting for docking to turn off the FMW motors after successful locking between OLEV and client S/C.

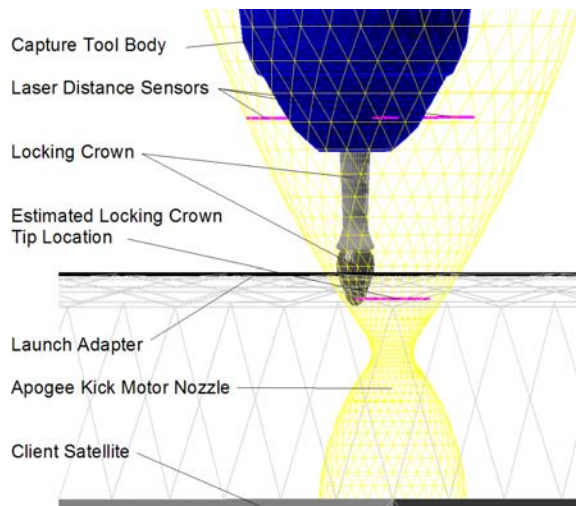


Figure 11: Initial Simulation Configuration

Beside the 3-axes stabilization, the client is additionally stabilized by a 4th loaded reaction wheel. The deployment of the Capture Tool is realized by a flexible telescopic boom with a deployment velocity range of +/- 4 mm/s. The success of docking depends strongly on the control algorithm of the Capture Tool deployment, respectively the boom deployment.

The underlying strategy is such, that the deployment velocity will be significantly reduced if

physical contact between the Capture Tool or its Locking Crown and the nozzle is expected. Then, the contact energy can be minimized. And following, the boom drive is able to superpose the passive lateral motion caused by bouncing after contact with an active deployment motion such, that the trajectory of the Capture Tool tip travels without contact along the nozzle contour towards the nozzle throat.

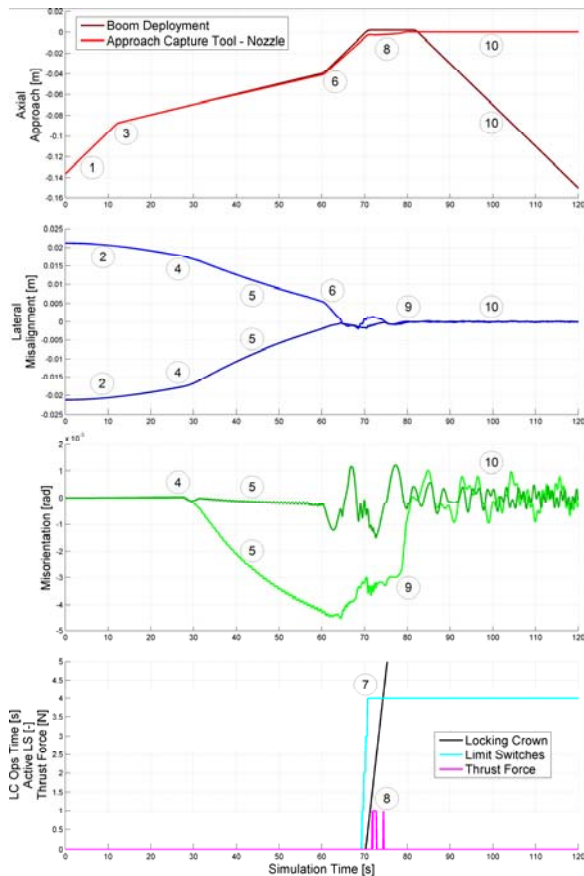


Figure 12: Capture Tool Approach During Docking

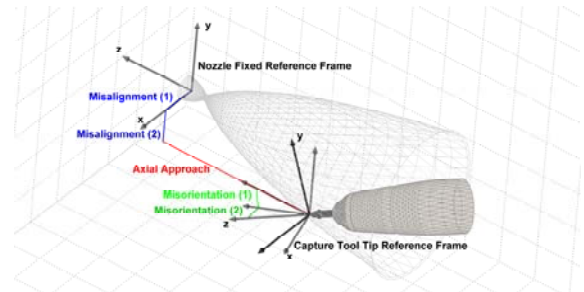


Figure 13: Legend for Capture Tool Approach

Table 1: Docking Protocol

- (1) The Capture Tool is being deployed with maximum velocity of 4 mm/s. No physical contact between the Capture Tool and the nozzle is expected.
- (2) The AOCS of SMART-OLEV reduces slightly the initial lateral misalignment.
- (3) The Capture Tool, respectively its Locking Crown is now close to the nozzle surface. The deployment velocity will be reduced to 1 mm/s in order to minimize the expected contact shock energy.
- (4) Physical contact between the Capture Tool and the nozzle takes place.
- (5) The Capture Tool tip bounces and moves laterally towards the nozzle center line. Caused by the torque of the contact shock the satellites start to turn. However, the FMWs at the client can minimize the amount of mis-orientation in one of the affected satellite axes.
- (6) The Capture Tool tip has reached the nozzle throat. For passing the throat the deployment velocity will be increased to 4 mm/s.
- (7) After passing the nozzle throat, four limit switches at the Capture Tool shoulder indicate that the Locking Crown has to be activated.
- (8) Since the measured approach velocity differs too much from the boom deployment velocity, the axial thrusters of SMART-OLEV fire with 1 N in order to correct this error.
- (9) The Locking Crown locks the client nozzle (see Figure 5). Lateral misalignment and angular mis-orientation disappear.
- (10) The locking force of the Locking Crown is about 100 N (see Figure 14). This amount is sufficient to keep the connection between Capture Tool and nozzle stiff enough during the boom retraction phase.

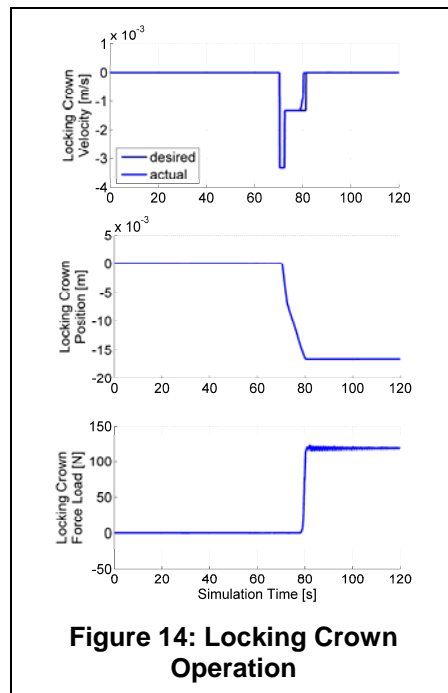


Figure 14: Locking Crown Operation

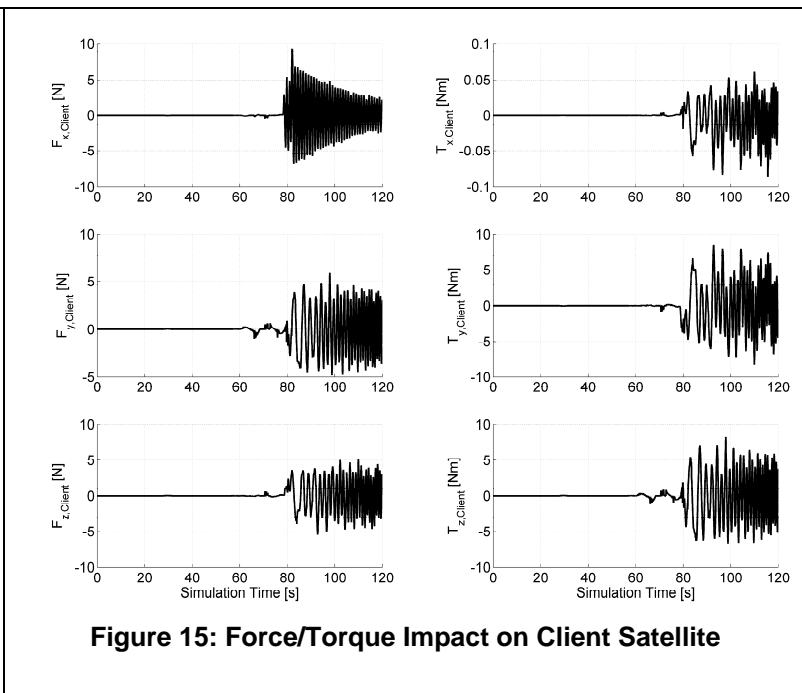


Figure 15: Force/Torque Impact on Client Satellite

The position of the Capture Tool tip can be derived from the radial measurements of the laser distance sensors mounted on the Capture Tool compared to a 3D-model of the nozzle used as reference. For passing the nozzle throat the deployment speed will be increased to its maximum. Four limit switches indicate the maximum penetration of the Capture Tool and activate the Locking Crown. This device will be spread quickly and retracted into the Capture Tool. Hereby, the nozzle will be locked and safely attached to the Capture Tool.

Now the critical phase of the docking is finished and the boom can be retracted in order to pull the client satellite against a dedicated support mechanism at the OLEV.

For safety reasons the docking strategy offers the option to activate axial thrust forces at OLEV. These are required to accelerate OLEV if the measured approach velocity differs too much from the boom deployment velocity.

4.2.1. Docking Simulation Results

The docking simulation results according to the scenario mentioned above are presented in Figure 12 with a protocol like discussion of the according function plots in Table 1. The legend in Figure 13 explains the meaning of the presented function plots. The presented results are representative for a large number of similar simulations, which were performed for OLEV phase B in order to prove the robustness of the proposed docking strategy. Concluding we can state that in all simulations the docking could be

finished successfully. It was proven, that the accuracy of the proposed sensors at the Capture Tool as well as the performance of the proposed boom and Locking Crown actuators (Figure 14) have been designed adequately.

Beside the kinematics aspect of the docking it is has to be proven that client satellite will not be damaged during the docking maneuver. According to the presented simulation results the force/torque impact at the client satellite (reference point = center of mass) is quite moderate (Figure 15). The actual amount of forces and torques is always lower than 10 N, respectively 10 Nm, which is definitively less than the applicable force/torque limits.

5. Acknowledgement

The RVD P/L Phase B activities have been co-funded by DLR within contract no. 50JR0562 and 50JR0664.

6. References

- [1] C. Kaiser, F. Sjöberg, J.-M. del Cura, B. Eilertsen: SMART-OLEV – An Orbital Life Extension Vehicle for Servicing Commercial Spacecrafts in GEO, 58th IAF Congress, 24.-28. September 2007, Hyderabad, India, IAF-Paper IAC-07-D1.1.06
- [2] G. Hippmann; “An Algorithm for Compliant Contact Between Complexly Shaped Surfaces in Multibody Dynamics”; *MULTIBODY DYNAMICS 2003*; IDMEC/IST, Lisbon, Portugal, July 1-4, 2003